An Estimate of Equatorial Upwelling in the Pacific[1]

KLAUS WYRTKI

Department of Oceanography, University of Hawaii, Honolulu 96822

(Manuscript received 20 February 1981, in final form 7 July 1981)

ABSTRACT

Upwelling in the equatorial Pacific Ocean manifests itself by a tongue of cool water stretching from the Galapagos Islands to the date line. To estimate the rate of upwelling, the mass, heat and salt budgets of the tongue are investigated. The Ekman divergence is determined from wind stress as 84×10^6 m^3 s^{-1}. It is compensated by geostrophic convergence of the same magnitude as determined from the zonal pressure gradient. Since the vertical distribution of the two meridional flows is different, a strong vertical circulation results, which leads to upwelling at a rate of $\sim 50 \times 10^6$ m^3 s^{-1}. A consideration of the heat budget leads to the conclusion that horizontal advection in the South Equatorial Current does contribute to the cool tongue, but that the contribution of upwelling is much larger. The heat budget also indicates that upwelling comes from depths above the core of the undercurrent and that the source water has temperatures only ~3°C less than the water flowing out laterally. The seasonal variation of all properties associated with the cool tongue is strong and produces a cross-equatorial flow of water from the summer to the winter hemisphere of $\sim 20 \times 10^6$ m^3 s^{-1}.

1. Introduction

The upwelling of cool subsurface water in the equatorial Pacific and the other oceans is well known (Cromwell, 1953; Knauss, 1963). Estimates have been made of the speed of the upwelling, but an estimate of the bulk rate of upwelling in terms of total volume of water for the entire upwelling area per unit time is still missing. Upwelling in the equatorial Pacific Ocean manifests itself by a tongue of cool water stretching from the coast of Peru to the date line. This tongue is partly caused by horizontal advection of cool water from the east and partly by upwelling. The entire upwelling area is subject to a mean annual heat gain, and consequently the heat budget will place important constraints on estimating the rate of upwelling. Upwelling is caused by the divergence of the Ekman flow at the equator, which is partly opposed by the convergence of geostrophic flow due to the general east-west slope of sea level along the equator.

The salt budget of the area is less well defined, as a strong north-south gradient of salinity exists across the equator and the upwelling area. In this study the mass, heat and salt balance of the upwelling area will be considered. Aspects of the geochemical budget have been discussed by Broecker *et al.* (1981) and Fine (1981). First, it will be necessary to define the upwelling area to identify the processes of importance and to establish boundaries for budget calculations.

2. The tongue of cool water along the equator

The mean annual variation of the shape and temperature of the cool tongue is best represented in the atlas by Robinson (1976), and Fig. 1 is redrawn from her atlas. The tongue stretches from the Galapagos Islands to the date line and forms a temperature minimum at the equator. East of 120°W the tongue may be situated slightly to the south of the equator. The tongue is usually connected to the cool upwelling water along the coast of Peru. To the north of the tongue is the warm tropical surface water of low salinity associated with the North Equatorial Countercurrent. During the entire year a surface temperature maximum of more than 26°C extends along 8°N from the western to the eastern Pacific Ocean coinciding with the Countercurrent. To the south the tongue is less sharply defined, but a ridge of maximum temperatures extends eastward along 8°S from the western Pacific to 90°W and beyond as seen in the temperature maps by Wyrtki (1964).

The tongue is best developed from August to October, when the southeast trade winds are strongest during southern winter. At this time, temperatures south of the Galapagos Islands are ~20°C, the tongue is clearly connected with the upwelling waters off Peru; the temperature minimum lies about 2° south of the Galapagos Islands and approaches the equator between 110 and 120°W. The east-west difference of temperature between the Galapagos Islands and the date line is 8°C. A well-defined temperature front near 3°N forms the northern boundary of the tongue. This front is

[1] Hawaii Institute of Geophysics Contribution No. 1182.

0022-3670/81/091205-10$06.50

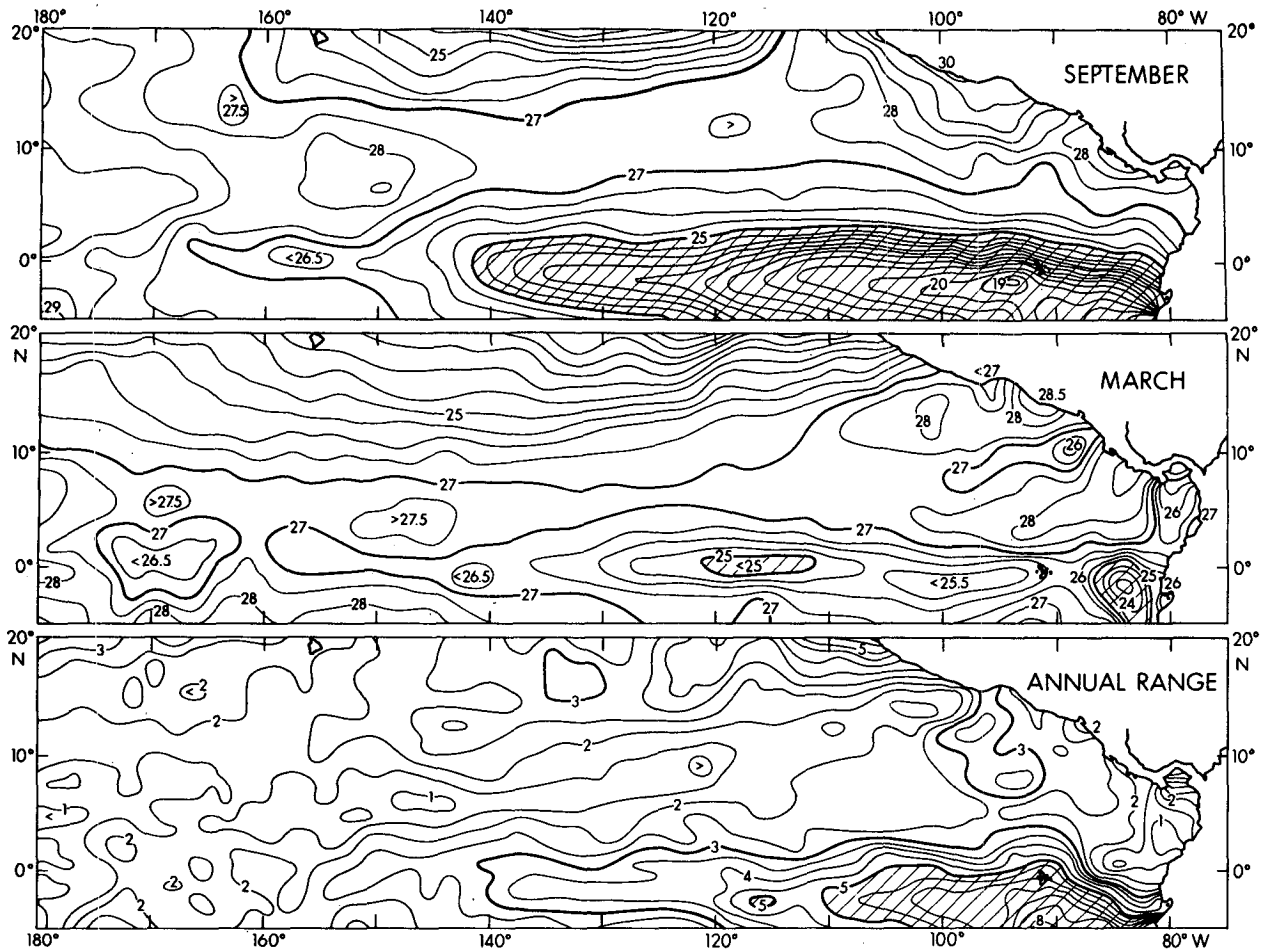

FIG. 1. The cool equatorial tongue as shown by the distribution of mean sea surface temperature in March and September and its annual range (according to Robinson, 1976).

strongest near the Galapagos Islands and decreases in strength westward. To the south, the meridional temperature gradient is much weaker.

The weakest development of the tongue is in February and March, during southern summer, when the southeast trade winds are weakest, at least over the eastern half of the tongue. At this time no clear connection seems to exist between the cool upwelling waters off Peru and the tongue, and often the warm waters north and south of the Galapagos Islands are connected by temperatures of more than 26°C. Farther west along the equator, especially between 110 and 120°W, lower temperatures below 25°C indicate upwelling. At this time the development of the tongue appears to be more symmetrical, since temperatures north and south of it are similar, although the differences are smaller.

West of the date line a temperature minimum can also be recognized on many temperature sections, but its magnitude is often <1°C, and an organized tongue can no longer be established in charts of mean monthly temperatures. This does not mean that upwelling is nonexistent to the west of the date line, but that the mixed layer is so thick that upwelling is not noticeable by an appreciable drop in sea surface temperature. Upwelling has, in fact, been documented to the west of the date line by Hisard *et al.* (1970).

The entire cool tongue lies in the South Equatorial Current, which flows westward at high speeds. Typical mean surface speeds are ~40 cm s^{-1} between the Galapagos Islands and 130°W (Wyrtki, 1965a). Farther west the mean speeds of the South Equatorial Current are somewhat smaller (U.S. Navy Hydrographic Office, 1950). The northern boundary of the current is near 5°N, north of which the North Equatorial Countercurrent flows in the opposite direction. The temperature front near 3°N is not coincident with the boundary between the two currents. The high speeds associated with the core of the South Equatorial Current extend to about 5°S, and speeds decrease southward until the South Equatorial Countercurrent is reached near 10°S.

Transports of the South Equatorial Current in the

upper 50 m are difficult to establish, but some estimates can be made. West of the Galapagos Islands the current is often shallow—only 30–50 m deep with a strong shear of velocity toward the undercurrent beneath (Knauss, 1966). Assuming a current speed of 40 cm s^{-1}, a width of 10^3 km and a depth of 30 m, a transport of only 12×10^6 m^3 s^{-1} results. Surely, the total transports of the South Equatorial Current are much larger than 12×10^6 m^3 s^{-1}, but would include transports farther away from the equator and flow below 30 m depth (Wyrtki, 1966). Recent direct measurements of currents near the equator during the NORPAX Hawaii to Tahiti Shuttle Experiment by Firing (1981) give mean transports of $\sim 20 \times 10^6$ m^3 s^{-1} between 3°N and 3°S for the South Equatorial Current between 150 and 158°W in 1979 and 1980. Near the date line the upper mixed layer is even deeper than at 150°W, its depth often exceeding 100 m and, consequently, the transports of the South Equatorial Current within the upper layer may actually increase from east to west.

3. Processes maintaining the tongue

The mass balance of the cool tongue is given by four components: 1) the horizontal advection of water in the South Equatorial Current; 2) the upwelling of water from below; 3) the lateral advection of water in the divergent Ekman layer; and 4) the convergence of geostrophic flow toward the equator (Fig. 2). The heat balance has four additional components, namely, the net surface heat input, the lateral diffusion of heat toward the center of the tongue, the vertical downward heat flux and the longitudinal eddy diffusion of heat, which is probably small compared with the other contributions.

In general, it can be argued that the tongue is maintained by advection of cold water from the east and by upwelling of cool water from below. The net heat input at the sea surface will warm these two contributions to allow an outflow of warm water with the South Equatorial Current in the west and a lateral outflow of warm water in the Ekman drift away from the equator. The contributions of cool advection and of upwelling as well as the heat input will vary throughout the year and result in the observed annual and interannual variations of the intensity of the tongue. It is the purpose of this study to estimate the magnitudes of the various contributions.

4. The model

A box model appears to be appropriate for this study so that the fluxes of mass, heat and salt across its sides can be estimated (Fig. 2). The length of the box will be given by the length of the cool tongue from the Galapagos Islands to the date line, which is 90° of longitude or 10^4 km. The actual locations of the eastern and western sides of the box have been chosen as 100°W and 170°E, because hydrographic data near these two meridians were used to calculate the east-west pressure gradient. The lateral boundaries of the box are more difficult to define. Upwelling on top of the undercurrent is probably restricted to ~2° of latitude from the equator. The width of the cool tongue, as measured by the maximum temperature gradient on either side, is ~3° to either side of the equator, and it is somewhat less in the north and more in the south. On the other hand, calculations of the Ekman transport, which is inversely proportional to latitude, only settle to reasonable values at a latitude of ~5°, as will be shown when discussing Fig. 3. Consequently, Ekman and geostrophic transport calculations have been made at 5°N and 5°S, and this will determine the width of the box as two times 550 km. The depth of the mixed layer increases along the equator from east to west from ~30 m near the Galapagos Islands to ~100 m near the date line (Robinson, 1976). The depth of the Ekman layer at very low latitudes is essentially unknown, but it may be assumed that it is less than the depth of the mixed

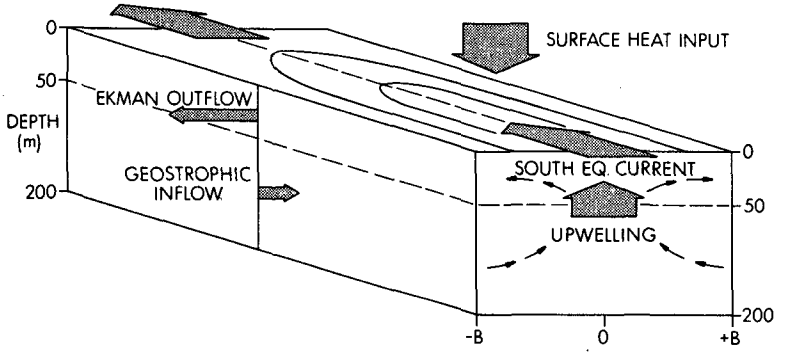

FIG. 2. Schematic view of the cool tongue along the equator, showing the major components of the mass and heat balance.

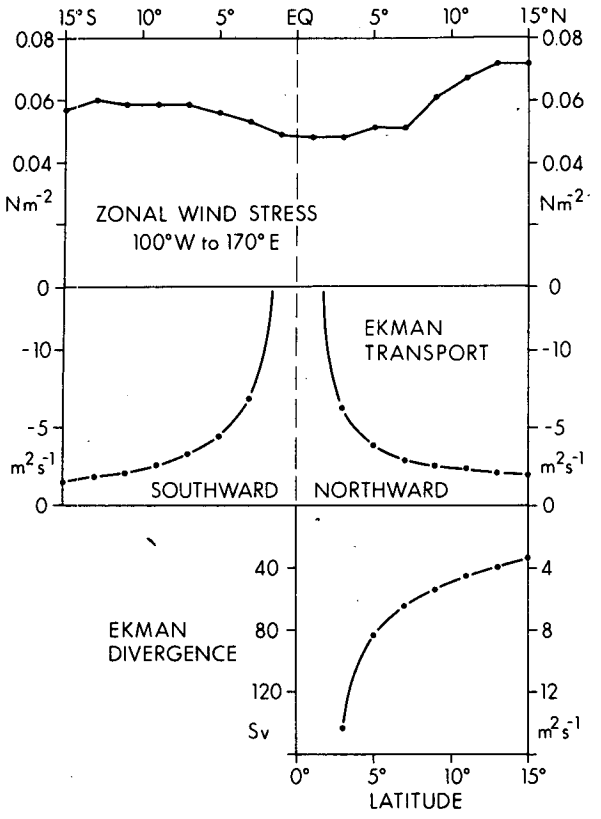

FIG. 3. Mean annual zonal wind stress, Ekman transport and Ekman divergence as a function of latitude between 100°W and 170°E in the equatorial Pacific Ocean. The Ekman divergence is also given in units of 10^6 m^3 s^{-1}.

layer. As it is desirable to make the box deeper than the Ekman layer but shallower than the thermocline, an average depth of 50 m has been chosen.

5. The Ekman transport

The zonal component of the wind stress τ^x causes the meridional Ekman transport V^y according to the relation $\rho f V^y = \tau^x$, where f is the Coriolis parameter and ρ the density of the water. Along the equator the southeast trade winds are essentially zonal except near the Galapagos Islands and, consequently, Ekman transport is away from the equator in either hemisphere, causing a strong divergence near the equator. A useful table of the average zonal wind stress over the Pacific Ocean for intervals of 2° of latitude has been given by Wyrtki and Meyers (1976), but the averages include the region of seasonally very weak winds between the date line and the Southeast Asian waters. Consequently, new averages have been computed from the original data for the area from 100°W to 170°E, a distance of 10^4 km. A meridional profile of the mean zonal wind stress, of the corresponding Ekman transport and of the divergence of the Ekman transport is shown in Fig. 3. The zonal wind stress has a weak minimum near 2°N and increases only slowly toward the core regions of the northeast and southeast trade winds. The Ekman transport and the Ekman divergence increase toward the equator inversely proportional to latitude; consequently, values close to the equator are unrealistic, because the simple Ekman balance no longer applies. Poleward of 4° of latitude, the curves settle to reasonable values. The Ekman transport at 5°N is 4.0 m^2 s^{-1}, and at 5°S it is 4.4 m^2 s^{-1}. The total Ekman divergence over a distance of 10^4 km is 84×10^6 m^3 s^{-1}. This value constitutes the divergence of the Ekman flow at 5° of latitude, but not the upwelling, because the divergence is partly offset by convergence of geostrophic flow toward the equator due to the east-west pressure gradient.

6. Equatorward geostrophic transport

In the equatorial Pacific Ocean dynamic height increases from east to west, and consequently, causes an equatorward geostrophic flow. Dynamic heights were computed for the area between 160 and 170°E for each interval of 2° of latitude. The number of stations in each of these areas was between 10 and 61. Dynamic heights were also computed along 95°W from a mean hydrographic section derived from all data between 94° and 96°W using a total of 121 stations (Lucas, 1981). The difference of dynamic height ΔD between 165°E and 95°W as a function of depth relative to 500 db is shown in Fig. 4. Between 3°N and 3°S the curves are virtually identical; the curve at 5°S embraces a somewhat larger area, the curve at 5°N a somewhat smaller area. To convert the zonal pressure gradient into meridional geostrophic flow, the Coriolis parameter at 5° of latitude, the same as in the Ekman calculations, is used, giving equatorward surface currents of 3–4 cm s^{-1}, which decrease almost linearly to 200 m depth. If, for reasons of symmetry, the pressure gradient between 3°N and 3°S is used to determine the equatorward geostrophic transport at the flanks of the upwelling region, an east-west distance of 100° of longitude and the Coriolis parameter at 5° of latitude, the total geostrophic transport is 42×10^6 m^3 s^{-1} from each side, of which 19×10^6 m^3 s^{-1} are in the upper 50 m.

This calculation implies that the geostrophic convergence in the upper 200 m of the equatorial region effectively balances the Ekman divergence, but because the vertical distribution of the two meridional flows is different a strong vertical circulation results, which leads to equatorial upwelling, as shown by Fofonoff and Montgomery (1955). The problem of the balance between Ekman divergence and geostrophic convergence at the equator has been addressed by Stommel (1960). He showed that

"there is indeed no singularity at the equator" and that "there is no reason to suppose that Ekman's solution 'blows up'." Whereas he applies his computations to the undercurrent, they may be much more relevant to equatorial upwelling, which is not even mentioned.

7. Equatorial upwelling

The estimates of Ekman divergence and of geostrophic convergence can now be combined to estimate the upwelling. The lateral outflow in the Ekman layer at 5°N is 40 × 10^6 m^3 s^{-1}, and at 5°S is 44 × 10^6 m^3 s^{-1}. If the zonal pressure gradient near the equator is used, but the Coriolis parameter at 5° of latitude, the resulting transports are as shown in Fig. 5A. The Ekman divergence of 84 × 10^6 m^3 s^{-1} is partially balanced by the geostrophic convergence of 38 × 10^6 m^3 s^{-1} in the upper layer. Below 50 m the geostrophic convergence is 46 × 10^6 m^3 s^{-1}, all of which is used for upwelling. If this upwelling mass flux is distributed evenly over a distance of 10^4 km east-west and of 400 km north-south, the resulting vertical upwelling velocity is 1.15 × 10^{-5} m s^{-1} or 1 m day^{-1}. The actual upwelling velocity at the equator may be much larger.

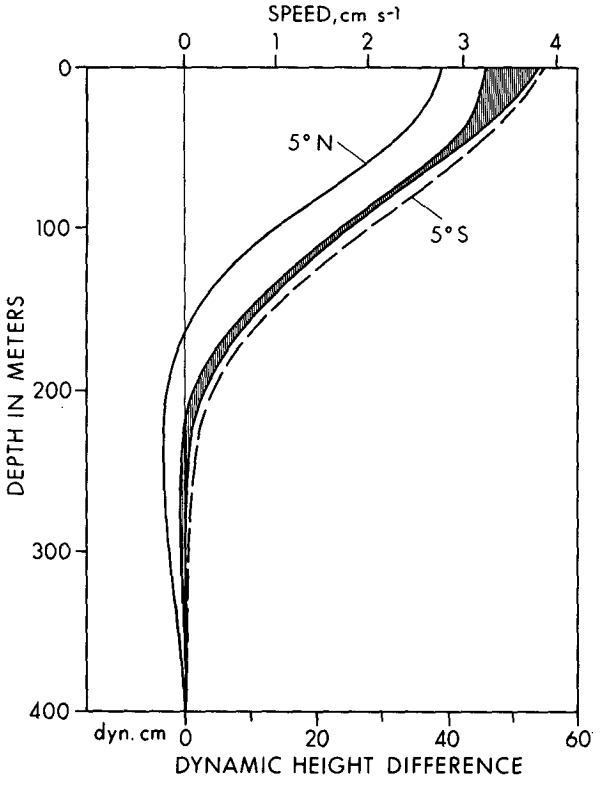

FIG. 4. Difference of dynamic height (dyn cm) between 95°W and 165°E as a function of depth. The curves at 5°N and 5°S are shown, the shaded area brackets the four curves between 3°N and 3°S.

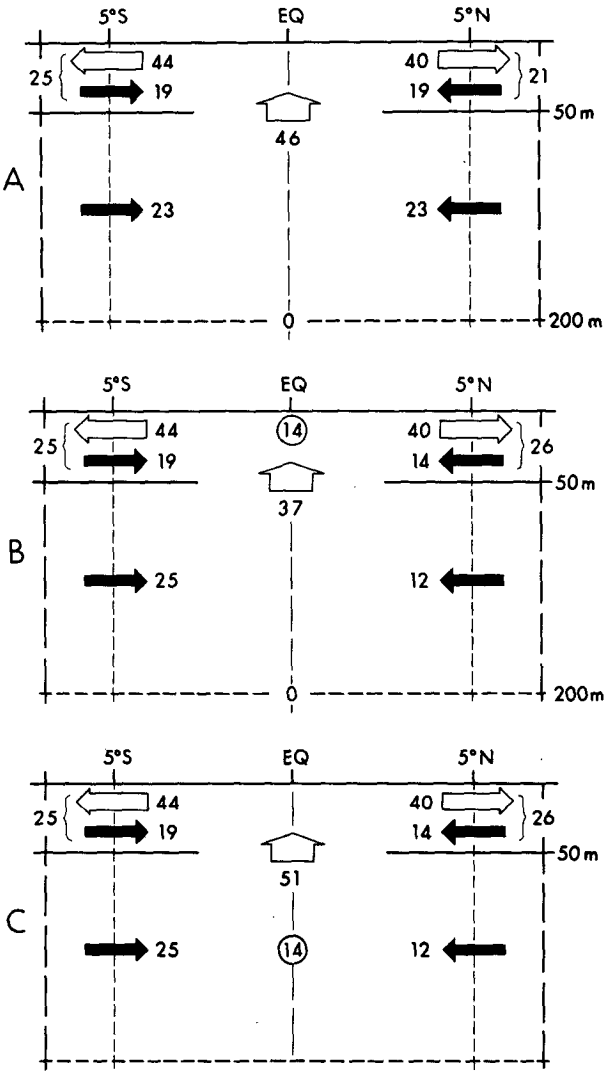

FIG. 5. Three cases of the water balance in the equatorial upwelling area between 5°N and 5°S. Flows are in units of 10^6 m^3 s^{-1}. The open arrows represent Ekman flow, the full arrows geostrophic flow. The upward arrow is upwelling and the circled number represents an east-west convergence. For a discussion see the text.

If the zonal pressure gradients at 5°N and 5°S are being used, the geostrophic flow is 26 × 10^6 m^3 s^{-1} from the north and 44 × 10^6 m^3 s^{-1} from the south. In this case the Ekman divergence is slightly larger than the geostrophic convergence and the deficit must come either from a convergence in the east-west flow of the South Equatorial Current or of the undercurrent. Fig. 5B shows the first case where an Ekman outflow of 84 × 10^6 m^3 s^{-1} is partially compensated by a geostrophic convergence of 33 × 10^6 m^3 s^{-1}. The subsurface convergence of 37 × 10^6 m^3 s^{-1} is entirely used for upwelling and, consequently, the remaining 14 × 10^6 m^3 s^{-1} must be provided by horizontal convergence in the South

Equatorial Current. In the second case, the entire divergence of the upper layer had to be compensated by upwelling of 51×10^6 m^3 s^{-1} (Fig. 5C). Since the geostrophic convergence in the subsurface layer is only 37×10^6 m^3 s^{-1}, the deficit of 14×10^6 m^3 s^{-1} would have to come from a convergence of the undercurrent or from below the undercurrent. The latter is unlikely to be the average situation, since downwelling rather than upwelling is indicated in the lower portion of the undercurrent by the downward deflection of the isotherms. A decrease of the transport of the undercurrent by 14×10^6 m^3 s^{-1} between the date line and the Galapagos Islands, on the other hand, is the most likely situation and is in agreement with existing knowledge.

The limiting case of maximum upwelling would, of course, be an extremely thin Ekman layer. The entire divergence of the Ekman layer would be compensated by upwelling of $\sim 80 \times 10^6$ m^3 s^{-1}, which in turn would be supplied by geostrophic convergence below the Ekman layer. The most likely case is probably the situation in Fig. 5C with $\sim 50 \times 10^6$ m^3 s^{-1} of upwelling, and part of the Ekman divergence being supplied by horizontal convergence in the equatorial undercurrent.

8. The heat balance

The heat budget of the upper layer is controlled by six processes: 1) the heat input at the sea surface; 2) the advection of cool water from the east; 3) the upwelling of cool water from below; 4) the meridional outflow of warm water in the Ekman layer; 5) the lateral turbulent heat flux toward the equatorial temperature minimum; and 6) the downward turbulent flux of heat into the thermocline. The magnitude of these six processes will first be estimated to show that the first four are all of nearly the same magnitude and, consequently, the heat balance of the upwelling area will decisively constrain the estimate of upwelling.

The equatorial Pacific Ocean between the Galapagos Islands and New Guinea is an area of net heat gain. The average annual heat input into the area given by 5°N, 5°S, 100°W and 170°E can be estimated from a map by Wyrtki (1965b) and is ~ 175 cal cm^{-2} day^{-1} or 85 W m^{-2}. For the total area this amounts to 202×10^{12} cal s^{-1} or 8.5×10^{14} W. More recent estimates by Hastenrath and Lamb (1978) for the eastern tropical Pacific and by Weare *et al.* (1980) give similar values of net heat gain within an estimated error of ~ 6 W m^{-2} (Hastenrath, 1980).

The South Equatorial Current carries cool water of ~22°C from the waters off Peru to the west. During its flow along the equator this water is warmed and leaves the area in the west with a temperature of ~28°C. Assuming a transport of 15×10^6 m^3 s^{-1} for the South Equatorial Current between 5°N and 5°S, the cool advection amounts to a heat demand of 90×10^{12} cal s^{-1} or 3.8×10^{14} W, roughly half the surface heat input.

Upwelling is another source of cool advection. Assuming that all upwelled water leaves the area laterally in the Ekman layer, the heat demand is given as the product of the upwelling rate W and the temperature difference ΔT between the upwelling water and the water leaving in the Ekman layer. With an upwelling rate of 50×10^6 m^3 s^{-1} and an average temperature difference of 4°C, the heat demand is 200×10^{12} cal s^{-1} or 8.4×10^{14} W, equal to the heat gain at the sea surface.

The only other heat gain of the upwelling area is the lateral turbulent heat flux toward the equatorial temperature minimum. Making the simple assumption that the meridional temperature profile between 5°N and 5°S is given by the equation $T(y) = \Delta T(1 - y^2/B^2)$, where ΔT is the temperature difference and B the distance between the equator and 5° of latitude, the resulting heat flux at 5°N is $\rho c_p K^h dT/dy = \rho c_p K^h \Delta T 2/B$, where K^h is a horizontal exchange coefficient, $\sim 10^7$ cm^2 s^{-1}. Using a temperature difference of 2°C, the resulting heat flux is 0.8 cal cm^{-2} s^{-1}. With a depth of 50 m for the upper layer and an east-west length of 10^4 km, the total heat flux toward the temperature minimum is 4×10^{12} cal s^{-1}, or about 16×10^{12} W from either side. This heat flux is small when compared to the other processes contributing to the heat budget. Only if the horizontal exchange coefficient were as high as 10^8 cm^2 s^{-1} would the contribution of lateral turbulent heat fluxes become comparable with the other processes. The zonal eddy heat flux along the tongue, of course, is much smaller than the meridional eddy heat flux and can be disregarded.

The heat flux entering at the sea surface will be rapidly distributed throughout the mixed layer and used to warm the water. The real question is how much of the heat escapes through the strong tropical thermocline. Recent measurements by Crawford and Osborn (1981) in the equatorial Pacific indicate that the equatorial regime of very high turbulent dissipation above the undercurrent core is confined within ~100 km of the equator. Above the undercurrent the downward turbulent flux of heat is balanced by the advective upward flux of cool water. In and below the core of the undercurrent, at depths from 140 to 280 m, the flow is almost laminar and the vertical eddy diffusivity is about $K^v = 0.02$ cm^2 s^{-1} (Osborn, 1980). Consequently, little heat escapes from the surface layer through the core of the undercurrent to deeper levels. Gregg (1976) states that the heat flux through

the velocity maximum of the undercurrent is about a factor of 10 less than that through the upper active region.

Off the equator (and this is the largest part of the area under consideration), the eddy diffusivity for heat in the thermocline is probably as low as $K^v = 0.1$ cm^2 s^{-1}. With a temperature gradient $dT/dz = 10°(100\text{ m})^{-1} = 10^{-3}$ °C cm^{-1}, the heat flux $\rho c_p K^v dT/dz$ equals 10^{-4} cal cm^{-2} s^{-1}. For the total area of the box of 10^{13} m^2 this gives a heat flux of 10^{13} cal s^{-1} or $\sim 4 \times 10^{13}$ W, which is small compared to the major terms in the heat budget. This result implies that virtually all of the heat flux entering at the sea surface is used to heat the ascending upwelling water, and that little penetrates downward through the thermocline.

The conclusion from this rough analysis is that the surface heat input can be balanced by either the horizontal advection or the upwelling, and that when both processes are active either one must be somewhat weaker than so far assumed.

9. The salt budget

The salt budget of the cool tongue is most difficult to establish, as a strong gradient of surface salinity exists perpendicular to the tongue. North of the tongue between 5 and 10°N, low-salinity tropical surface water extends from the western to the eastern Pacific with the Countercurrent and coincides with an area where precipitation exceeds evaporation by more than 0.5 m year^{-1} (Dietrich *et al.*, 1980) and salinities are less than 34.5‰. At the equator and to the south of it, evaporation exceeds precipitation and surface salinity increases systematically toward the subtropics where the evaporation excess is about 1 m year^{-1} and salinities are more than 36.0‰. Consequently, not only surface salinity has a pronounced north-south gradient, but also the forcing function, namely, the difference between evaporation and precipitation. The water advected from the region off Peru has a salinity of about 34.8‰, intermediate between that of the former two water masses. Salinity increases slightly from east to west along the tongue, which may either be an effect of the excess of evaporation over precipitation or of the upwelling of saltier water from the undercurrent, which has salinities between 35.0 and 35.5‰ in its core. A simple calculation for a box model shows that the mean salinities of the various fluxes must be known to 0.01‰, if the transports are to be estimated to 1×10^6 m^3 s^{-1}. This, of course, is impossible and, consequently, no worthwhile information or limiting conditions can be derived from the salt budget. One can, however, state that the observed salt distribution is at least not in conflict with the circulation scheme shown in Fig. 5.

A closer inspection of cross-equatorial salinity sections like those obtained during the NORPAX Test Shuttle Experiment (Taft and Kovala, 1979) shows that near a depth of 150 m, a tongue of high-salinity water of subtropical origin penetrates equatorward from the south. At the same depth, water of low salinity approaches the equator from the north. This water of North Pacific origin can be recognized as a salinity minimum only to ~5°N. These two components mix and provide upwelling water of an intermediate salinity. It is unlikely that water from below the undercurrent participates in the upwelling because much lower salinities would then be observed at the sea surface near the equator. Moreover, not only isotherms, but also isohalines between depths of 250 and 400 m are bent downward between 5°N and 5°S, indicating downward movements below the undercurrent. The surface water leaving from the equatorial upwelling region decreases in salinity as it moves north into a region of excess rainfall, and increases in salinity to the south as it moves into a region of excess evaporation.

10. The two limiting cases

Assuming that the heat input at the sea surface is completely absorbed by advection of cool water from the east with the South Equatorial Current, and that no upwelling takes place, gives the limiting condition for the strength of this current. In this case the cool tongue would be maintained entirely by advection and the governing condition is $\rho c_p U(T_0 - T_i) = Q$ where U is the volume transport of the South Equatorial Current, T_i and T_0 the temperatures at its western and eastern end, and Q the total heat input at the sea surface. With $T_0 = 28$°C, $T_i = 23$°C and $Q = 8.5 \times 10^{14}$ W, the transport is 40×10^6 m^3 s^{-1}. This transport is much larger than that determined from surface currents or direct measurements as discussed above and, consequently, the tongue is not maintained exclusively by advection, but upwelling also must contribute.

The other limiting case involves a complete balance between surface heat input and upwelling, according to the condition $c_p W(T_0 - T_u) = Q$, where W is the rate of upwelling and T_u the temperature of the upwelling water. The latter is most difficult to determine and is the biggest source of uncertainty in this estimate. Assuming that the temperature of the upwelling water at its source is 4°C colder than the temperature of the outflowing water, the maximum rate of upwelling is 50×10^6 m^3 s^{-1}. This is exactly the rate of upwelling established from the mass balance in Fig. 5. A temperature difference of only 4°C is consequently the maximum possible difference between the

divergent surface flow and the convergent subsurface flow feeding the upwelling. If horizontal advection in the surface layer plays any role, then this temperature difference should be less, probably only 3°C. Such a small difference implies that upwelling comes from very shallow depths near the top of the undercurrent and that much of the water converging laterally toward the equator is actually from the lower portions of the mixed layer. This assumption is not unreasonable since the depth of the Ekman layer is shallow, <50 m and, consequently, the bulk of the geostrophic convergence occurs immediately below the Ekman layer at depths between 50 and 100 m. At these depths temperatures are well above 20°C. Moreover, the water leaving the upwelling area in the Ekman layer to the south during the peak of the upwelling between June and October has a temperature much lower than the 28°C assumed for the outflow.

Direct measurements of equatorial currents made by Firing *et al.* during the NORPAX Hawaii to Tahiti Shuttle Experiment (Wyrtki *et al.*, 1981) were kindly made available to me. The average meridional component of the velocity and the average temperatures of all 41 sections at 3°N and 3°S were used to compute the mean meridional transports of mass and heat. At 3°N a poleward transport of 10.8 m^2 s^{-1} carries water with a mean temperature of 27.0°C in the upper 75 m. Below 75 m the equatorward flow is 4.5 m^2 s^{-1} and carries water of 22.8°C. In contrast, the poleward surface flow at 3°S is only 20 m thick and carries only 0.8 m^2 s^{-1}, but transports water of 28.0°C. The subsurface equatorward flow reaches to 160 m, and transports 6.3 m^2 s^{-1} at a mean temperature of 24.1°C. These computations result in a divergence of 11.6 m^2 s^{-1} in the surface layer and a convergence of 10.8 m^2 s^{-1} in the subsurface layer and compare favorably with the values given in Fig. 3. There is no obvious explanation for the asymmetry of the flow since it is averaged over one year, but it is at least in general agreement with Fig. 4, giving a stronger geostrophic flow from the south than from the north. The temperature difference between the in- and outflowing water is about 4°C on both sides of the upwelling area, but these measurements were made between 150 and 158°W, and may not be representative of conditions farther east.

11. The likely case and its problems

Taking both upwelling W and horizontal advection U into account, the heat balance equation is

$$W(T_0 - T_u) + U(T_0 - T_i) = Q/\rho c_p.$$

Using $T_0 - T_u = 3$°C and $T_0 - T_i = 5$°C, the relation reduces to $3W + 5U = 200$. With an upwelling of 50×10^6 m^3 s^{-1} as determined earlier from the mass balance, a flow of 10×10^6 m^3 s^{-1} results for the South Equatorial Current, being the lower of the estimates given in Section 2. In contrast, the estimate of upwelling seems somewhat high. The weakest assumptions in this balance are the temperature difference between the convergent and the divergent meridional flows and the choice of the Coriolis parameter for the computation of the mass balance. One would prefer to use the pressure gradient between 3°N and 3°S, so that the geostrophic convergence from both hemispheres is equal and balances exactly the Ekman divergence, but using a Coriolis parameter at 3° of latitude for the Ekman computations is just unrealistic. On the other hand, being consistent and using pressure gradients and Coriolis parameter at 5° of latitude results in an imbalance between Ekman divergence and geostrophic convergence, requiring a convergent equatorial undercurrent, which is, of course, possible.

Using this higher value of upwelling on the other hand requires a very small temperature difference between the divergent surface flow and the convergent subsurface flow feeding the upwelling. It is possible, but not certain that this difference is as low as determined here. The low temperature difference, in turn, indicates that temperatures along the equator should be rather sensitive to variations in the intensity of upwelling, and consequently of the winds, a fact which has been well known (Bjerknes, 1966).

12. Seasonal variations of upwelling

The trade winds over the cool tongue are subject to a sizable annual fluctuation, in particular along the northern flank of the tongue (Fig. 6). Northward Ekman transport is largest in February when the northeast trades reach far south, and southward Ekman transport is largest in July and August when the southeast trades reach maximum strength over the equator. The sum of the two components gives the total Ekman upwelling, which is stronger than average between December and April and weaker than average from September to November. The low value in May appears to be an artifact arising from the lack of smoothing of the two original curves. The difference between the northward and the southward Ekman transport indicates a strong annual signal of transequatorial Ekman transport. Flow is from the summer to the winter hemisphere and has an amplitude of ~2 m^2 s^{-1} or $\sim 20 \times 10^6$ m^3 s^{-1}, relative to a net southward transport of only 4×10^6 m^3 s^{-1}.

In contrast to the wind field, with its large annual fluctuations, the geostrophic convergence will vary much less, because a strong difference of the east-west slope of the thermocline between 5°N and 5°S is difficult to generate. Consequently the geostrophic

convergence toward the equator will remain approximately equal from both hemispheres throughout the year. As a result the upwelled water will preferably go to the winter hemisphere, while the supply of upwelled water comes from both hemispheres. The return flow necessary to maintain the mass balance of each hemisphere occurs probably at greater depth.

A cross-equatorial heat flux also has been reported by Oort and Vonder Haar (1976) and recently computed in a model by Bryan and Lewis (1979). Bryan (1980) quotes a transport of $\sim 12 \times 10^{14}$ W from the summer to the winter hemisphere in the Pacific. A transport of 20×10^6 m^3 s^{-1} would transfer heat at a rate of 12×10^{14} W into the winter hemisphere, if the return mass flux would have a temperature at least 12°C lower than the surface flow. As the surface temperature is near 27°C, the return flow should have a temperature of 15°C, which implies that it occurs in the lower parts of the undercurrent, which is very unlikely; it probably occurs deeper, at lower temperatures.

13. Comparison with direct observations

The actual speed of upwelling cannot be measured directly, but Halpern (1980) has determined it from the divergence of measured horizontal flow in an array of four current meters at the equator near 110°W during a period of three months. He found upwelling between the surface and 125 m with a maximum upwelling speed of 3×10^{-5} m s^{-1} at a depth of 50 m. This value of ~ 2.5 m day^{-1} is more than the mean value of upwelling of 1 m day^{-1} determined here, but it was measured at the equator where the highest value can be expected. Burkov (1980) calculated upwelling of 2–3 m day^{-1} for the equatorial Pacific.

The northward drift of water has been measured by many drifting buoys in recent years. Patzert (1980) reported an average northward drift of 4 cm s^{-1} derived from buoys drogued at 30 m. The northward component of this drift is rather uniform from the equator to 20°N, although the buoys travel first to the west with the South Equatorial Current, then to the east with the Countercurrent and later again to the west with the North Equatorial Current. A drift of 4 cm s^{-1} over a depth of 50 m gives a transport component of 2 m^2 s^{-1}, a value comparable to the net northward flow of water shown in Fig. 5. The numerical value of this drift is similar to that derived by Stidd (1975) from ship drift observations.

Evidence for subsurface geostrophic flow toward the equator is given by the salinity distribution, but recent data on the distribution of tritium allow an independent confirmation of this flow. Fine and Ostlund (1980) show that a tongue of high tritium content approaches the equator from the north at

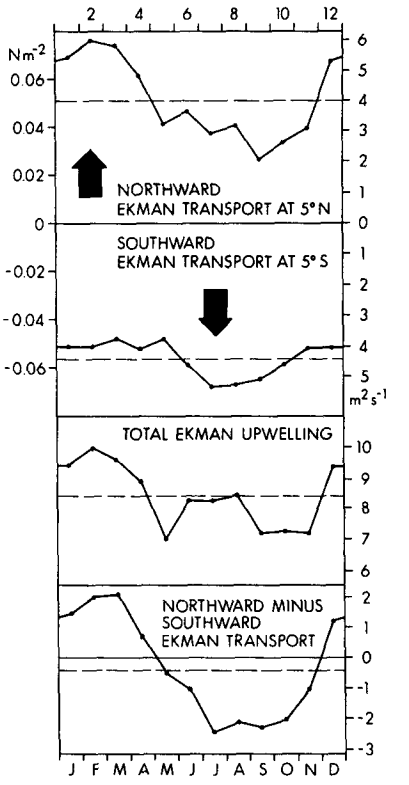

FIG. 6. Mean annual variation of zonal wind stress and poleward Ekman transports at 5°N and 5°S, their sum and difference. The dashed lines give the means.

isopycnal surfaces between sigma-theta of 24–25 kg m^{-3}. This density interval corresponds just north of the equator to the temperature interval between 19 and 23°C, but this water occupies only a very thin layer. It is further evidence that the geostrophic convergence and, consequently, the source of the upwelling water comes from shallow depths at rather high temperatures near the core of the undercurrent, but the measurements do not allow the computation of a rate for advection.

An attempt to determine the upwelling rate on the basis of bomb radiocarbon distribution in the Atlantic Ocean has been made by Broecker *et al.* (1978). They estimate a mean upwelling of 17 $\times 10^6$ m^3 s^{-1} for the equatorial Atlantic between 15°N and 15°S at a depth of 100 m. This is, of course, an area much larger than that occupied by upwelling along the equator above the undercurrent as defined in this study. Their area would include parts of the upwelling along the coast of Northwest Africa and in the Gulf of Guinea, and consequently their value for the upwelling cannot be compared directly with the estimate made in this study.

In numerical models of global ocean circulation the cool tongue along the equator is rarely developed in a manner comparable with observations. The computations by Takano (1975) show a tongue

almost 2000 km wide and stretching all the way to New Guinea. The model by Bryan *et al.* (1975) shows virtually no tongue at all. Consequently, it will be necessary to develop a specific model with a time-dependent wind stress and heat input and appropriate boundary conditions for the simulation of the cool tongue and of equatorial upwelling. The proper representation of important features of the ocean structure like this cool tongue should be a critical test for the quality of numerical models of ocean circulation.

Acknowledgments. I thank M. Cane, M. Gregg, G. Meyers and W. Patzert for valuable discussions and comments. This research has been supported by the National Science Foundation under the North Pacific Experiment of the International Decade of Ocean Exploration; this support is gratefully acknowledged.

REFERENCES

Bjerknes, J., 1966: A possible response of the atmospheric Hadley Circulation to equatorial anomalies of ocean temperature. *Tellus*, **18**, 820–829.

Broecker, W. S., T. H. Peng and M. Stuiver, 1978: An estimate of the upwelling rate in the equatorial Atlantic based on the distribution of bomb radiocarbon. *J. Geophys. Res.*, **83**, 6179–6186.

——, T. Takahashi, P. Quay and Dave Bos, 1981: Carbon dioxide and radiocarbon budgets for the equatorial Pacific Ocean. Submitted to *J. Geophys. Res.*

Bryan, K., 1980: Seasonal variation of poleward heat transport. *Ocean Modelling*, Vol. 33, 1–2.

——, and L. J. Lewis, 1979: A water mass model of the world ocean. *J. Geophys. Res.*, **84**, 2503–2517.

——, S. Manabe and R. Pacanowski, 1975: A global ocean-atmosphere climate model, Part II, the oceanic circulation. *J. Phys. Oceanogr.*, **5**, 30–46.

Burkov, V. A., 1980: *General Circulation of the World Ocean*. Gidrometeoizdat, 253 pp.

Crawford, W., and Thomas R. Osborn, 1981: Control of equatorial ocean currents by turbulent dissipation. *Science*, **212**, 539–540.

Cromwell, T., 1953: Circulation in a meridional plane in the central equatorial Pacific. *J. Mar. Res.*, **12**, 196–213.

Dietrich, G., K. Kalle, W. Krauss and G. Siedler, 1980: *General Oceanography. An Introduction*. John Wiley and Sons, 623 pp.

Fine, R. A., and G. Östlund, 1980: Exchange times in the Pacific equatorial current system. *Earth Planet. Sci. Lett.*, **49**, 447–452.

——, J. Reid and H. Östlund, 1981: Circulation of tritium in the Pacific Ocean. *J. Phys. Oceanogr.*, **11**, 3–14.

Firing, E., 1981: Current profiling in the NORPAX Tahiti Shuttle. *Trop. Ocean-Atmos. Newslett.*, **5**, 1.

——, C. Fenander and J. Miller, 1981: Profiling current meter measurements from the NORPAX Hawaii to Tahiti Shuttle Experiment. University of Hawaii, HIG Data Rep. No. 39, 146 pp.

Fofonoff, N., and R. Montgomery, 1955: The equatorial undercurrent in the light of the vorticity equation. *Tellus*, **7**, 518–521.

Gregg, M. C., 1976: Temperature and salinity microstructure in the Pacific equatorial undercurrent. *J. Geophys. Res.*, **81**, 1180–1196.

Halpern, D., 1980: Vertical motion at the equator in the eastern Pacific (abstract). *EOS*, **61**, 998.

Hastenrath, S., 1980: Heat budget of tropical ocean and atmosphere. *J. Phys. Oceanogr.*, **10**, 159–170.

——, and P. J. Lamb, 1978: *Heat Budget Atlas of the Tropical Atlantic and Eastern Pacific Ocean*. University of Wisconsin Press, 90 pp.

Hisard, P., J. Merle and B. Voituriez, 1970: The equatorial undercurrent at 170°E in March and April 1967. *J. Mar. Res.*, **28**, 281–303.

Knauss, J. A., 1963: Equatorial current systems. *The Sea*, Vol. 2, M. N. Hill, Ed., John Wiley and Sons, 235–252.

——, 1966: Further measurements and observations on the Cromwell Current. *J. Mar. Res.*, **24**, 205–240.

Lucas, R., 1981: Termination of eastward flow in the eastern equatorial Pacific. Ph.D. thesis, University of Hawaii (in preparation).

Oort, A. H., and T. H. Vonder Haar, 1976: On the observed annual cycle in the ocean-atmosphere heat balance over the Northern Hemisphere. *J. Phys. Oceanogr.*, **6**, 781–800.

Osborn, T. R., 1980: Estimates of the local rate of vertical diffusion from dissipation measurements. *J. Phys. Oceanogr.*, **10**, 83–89.

Patzert, W. C., 1980: Variability of tropical Pacific currents during 1979 and 1980 using drifting buoys (abstract). *EOS*, **61**, 997.

Robinson, M. K., 1976: *Atlas of North Pacific Ocean Monthly Mean Temperatures and Mean Salinities of the Surface Layer*. Naval Oceanogr. Office, Ref. Pub. 2, 173 figs.

Stidd, C. K., 1975: Meridonal profiles of ship-drift components. *J. Geophys. Res.*, **80**, 1679–1682.

Stommel, H., 1960: Wind-drift near the equator. *Deep-Sea Res.*, **6**, 298–302.

Taft, B. A., and P. Kovala, 1979: Temperature, salinity, themosteric anomaly and zonal geostrophic velocity sections along 150°W from NORPAX Shuttle Experiment (1977–1978). University of Washington, Special Rep. No. 87, Ref. M79-17, 28 pp.

Takano, K., 1975: A numerical simulation of the world ocean circulation: Preliminary results. *Numerical Models of Ocean Circulation*, R. O. Reid, A. R. Robinson and K. Bryan, Eds., Nat. Acad. Sci., 121–129.

U.S. Navy Hydrographic Office, 1950: *Atlas of Surface Currents, Northwestern Pacific Ocean*. 1st ed., H. O. Publ. 569, 12 pp.

Weare, B. C., P. T. Strub and M. D. Samuel, 1980: Marine Climate Atlas of the Tropical Pacific Ocean. University of California, Davis, Contribution No. 20, 146 pp.

Wyrtki, K., 1964: The thermal structure of the eastern Pacific Ocean. *Dtsch. Hydrogr. Z.*, Ergänzungsheft, Suppl. A, No. 6, 84 pp.

——, 1965a: Surface currents of the eastern tropical Pacific Ocean. *Dtsche. Hydrogr. Z.*, Ergänzungsheft, Suppl. A, 304.

——, 1965b: The average annual heat balance of the North Pacific Ocean and its relation to ocean circulation. *J. Geophys. Res.*, **70**, 4547–4559.

——, 1966: Oceanography of the eastern equatorial Pacific Ocean. *Oceanogr. Mar. Biol. Ann. Rev.*, **4**, 33–68.

——, and G. Meyers, 1976: The trade wind field over the Pacific Ocean. *J. Appl. Meteor.*, **15**, 698–704.

——, E. Firing, D. Halpern, R. Knox, G. J. McNally, W. C. Patzert, E. D. Stroup, B. A. Taft and R. Williams, 1981: The Hawaii to Tahiti shuttle experiment. *Science*, **211**, 22–28.